RESEARCH ARTICLE

NANO · MICRO small
www.small-journal.com

Light and Heat-Driven Flexible Solid Supramolecular Polymer Displaying Phosphorescence and Reversible Photochromism

*Wen-Wen Xu, Yong Chen, Xiufang Xu, and Yu Liu**

Herein, a type of light- and heat-driven flexible supramolecular polymer with reversibly long-lived phosphorescence and photochromism is constructed from acrylamide copolymers with 4-phenylpyridinium derivatives containing a cyano group (P-CN, P-oM, P-mM), sulfobutylether-β-cyclodextrin (SBCD), and polyvinyl alcohol (PVA). Compared to their parent solid polymers, these flexible supramolecules based on the non-covalent cross-linking of copolymers, SBCD, and PVA efficiently boost the phosphorescence lifetimes (723.0 ms for P-CN, 623.0 ms for P-oM, 945.8 ms for P-mM) through electrostatic interaction and hydrogen bonds. The phosphorescence intensity/lifetime, showing excellent responsiveness to light and heat, sharply decreased after irradiation with a 275 nm flashlight or sunlight and gradually recovered through heating. This is accompanied by the occurrence and fading of visible photochromism, manifesting as dark green for P-CN and pink for P-oM and P-mM. These reversible photochromism and phosphorescence behaviors are mainly attributed to the generation and disappearance of organic radicals in the 4-phenylpyridinium derivatives with a cyano group, which can guide tunable luminescence and photochromism.

1. Introduction

Stimuli-responsive materials with organic room-temperature phosphorescence (RTP) and photochromism are highly attractive owing to their advantages of facile preparation, long lifetimes, and dynamic optical changes, and have been commonly applied in the fields of photoelectric devices,[1,2] sensors,[3] bioimaging[4–6], and anti-counterfeiting.[7] Diverse strategies have been explored to obtain excellent RTP and photochromic materials. For instance, crystal strategies,[8] polymerization effects,[9] host–guest doping,[10] supramolecular assembly,[11–13] etc.[14–16] are useful methods for achieving purely organic RTP. In these strategies, various nonradiative relaxation pathways are greatly suppressed, and intersystem crossing (ISC) from excited singlet state to triplet state is obviously improved, thus resolving the inherent drawbacks of multiple nonradiative deactivations and weak spin-orbital coupling of some organic compounds. Photochromism, another photoresponsive property based on excited electrons, is characterized by a color change in appearance under light irradiation. Most photochromic materials consist of organic–inorganic hybrid components with effective charge transfer from the organic ligand to the metal center.[17–20] Additionally, some special light-driven organic reactions have also been utilized as photochromic units, such as the photocyclization of diarylethene,[21,22] photoreaction of tetraphenylethylene derivatives,[3,23] light-induced ring-opening and ring-closing of spiropyran,[24,25] and others.[26–30] Although phosphorescence and photochromism can be achieved selectively using different methods, organic materials possessing both RTP and photochromism faces forbidden challenges owing to the incompatible photophysical properties of most organic molecules.

In 2020, Bo and coworkers synthesized phthalic acid derivatives to achieve effective RTP with a lifetime of 428.6 ms in solid powder.[31] They used norbornyl to reduce the π–π distances and synergistically intensify the intermolecular interactions, achieving reversible photochromism and phosphorescence. In the following year, Li and coworkers reported that phosphorescence or photochromism could be realized separately by controlling aryl substituents based on triphenylamine derivatives.[32] Subsequently, the same group investigated the multi-photoresponsive properties of various triphenylethylene derivatives via organic photocyclization reactions, including photochromism, photodeformation, and RTP.[33] These excellent examples effectively validate the possibility of integration of phosphorescence and photochromic properties into one organic system.[34] However, most of these studies involved crystals or solutions based on organic photoreactions.[35–37] To the best of our knowledge, controlling reversible phosphorescence and photochromism through the generation and disappearance of organic radicals driven by light and heat has not been reported, although we reported that

W.-W. Xu, Y. Chen, X. Xu, Y. Liu
College of Chemistry
State Key Laboratory of Elemento-Organic Chemistry
Nankai University
Tianjin 300071, P. R. China
E-mail: yuliu@nankai.edu.cn

Y. Liu
Collaborative Innovation Center of Chemical Science and Engineering
Tianjin 300071, P. R. China

The ORCID identification number(s) for the author(s) of this article can be found under https://doi.org/10.1002/smll.202311087

DOI: 10.1002/smll.202311087

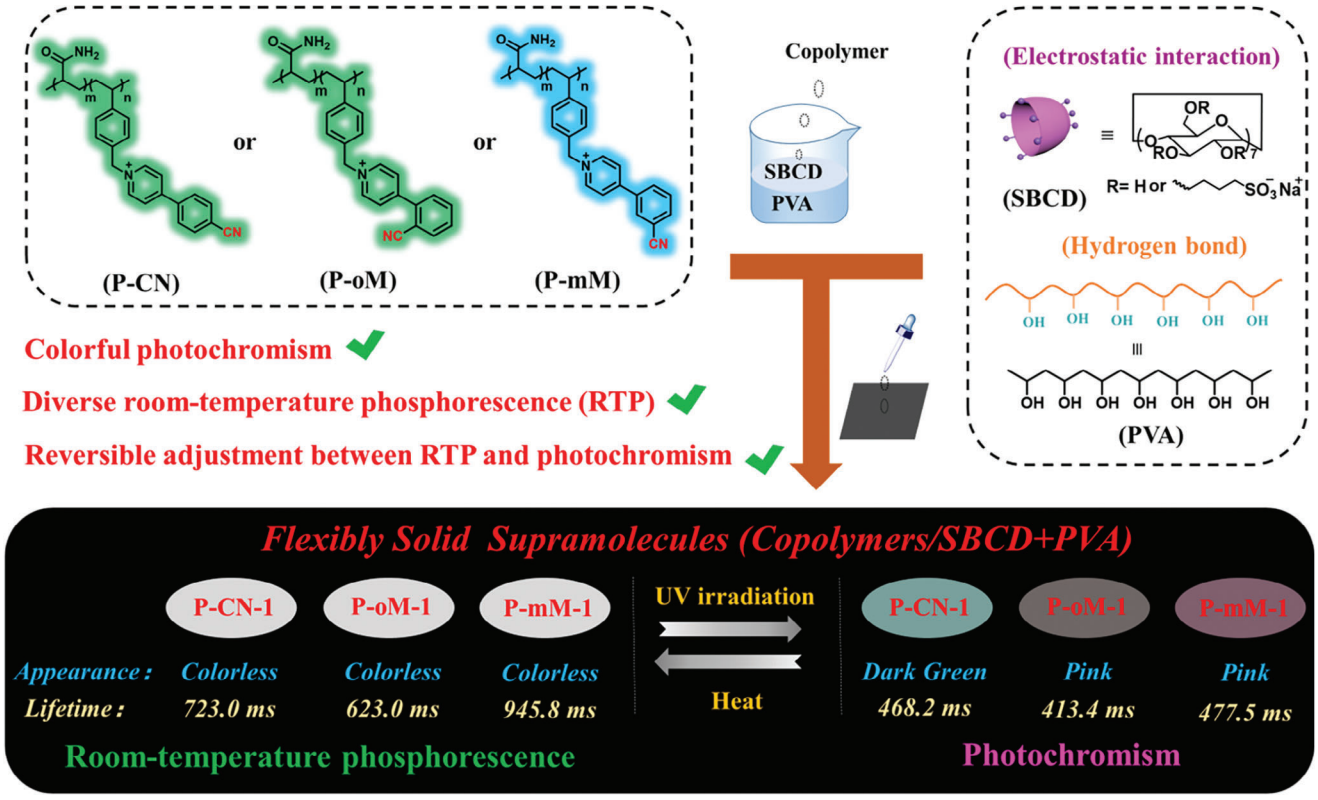

Scheme 1. Schematic illustration of light- and heat-driven flexible solid supramolecular polymer displaying phosphorescence and reversible photochromism.

macrocyclic confinement and polymerization synergistically promoted phosphorescence emission.[38]

In this study, reversibly long-lived room-temperature phosphorescence and colorful photochromism are achieved using solid acrylamide copolymers and supramolecular films based on copolymers, sulfobutylether-β-cyclodextrin (SBCD), and polyvinyl alcohol (PVA) (**Scheme 1**). The 4-phenylpyridinium derivatives containing a cyano group were copolymerized with acrylamide via binary radical polymerization reactions to obtain acrylamide copolymers (P-CN, P-oM, and P-mM). In particular, the resulting copolymers emitted bright RTP and exhibited colorful photochromism under UV irradiation. By tuning the cyano substituent on the benzyl group in 4-phenylpyridinium, the copolymers showed various lifetimes (514.4 ms for P-CN, 638.9 ms for P-oM, and 1056.4 ms for P-mM) and different photochromic appearances (dark green for P-CN and pink for P-oM and P-mM). After assembling with SBCD through electrostatic interaction and PVA through abundant hydrogen bonds, transparent, and processable films were obtained, and the phosphorescence lifetimes were further prolonged. Notably, the RTP and photochromic performance showed prominent reversibility in response to light and heat. The photochromic property gave copolymers and films a dark green or pink appearance; meanwhile, the intensity and lifetimes of RTP sharply decreased, and the duration of afterglow was obviously shortened. By heating the photochromic samples, their phosphorescent properties recovered, and colorless, transparent films were re-acquired. This was mainly due to the formation or disappearance of the radical state of the 4-phenylpyridinium derivatives in the materials induced by UV irradiation or heat. Notably, the same reversible photophysical behavior was also observed under sunlight, which endows this type of material with great potential for application in UV-blocking sunglasses and films, as well as sunlight-responsive smart optical materials.

2. Results and Discussion

2.1. Photochromic and Phosphorescent Copolymers

The 4-phenylpyridinium derivatives bearing a cyano group as chromophores (CN–V, oM–V, and *mM–V*), which were prepared through nucleophilic substitution between 4-phenylpyridine and 1-(chloromethyl)-4-vinylbenzene, only fluoresced with serrated emission and weak phosphorescence under shorter excitation wavelengths due to multiple deactivation pathways (vibration, rotation, collision, etc.) (Figures S1–S4, Supporting information). After copolymerization with acrylamide (P-CN, P-oM, and P-mM), the nonradiative pathways were inhibited, and long-lived room-temperature phosphorescence and colorful photochromic behaviors were unlocked. Photophysical properties, particularly phosphorescence, are closely related to the degree of chromophore substitution in copolymers.[39] Herein, copolymers with varying molar ratios of 4-(4-cyanophenyl)−1-(4-vinylbenzyl)pyridin-1-ium chloride were synthesized (namely, P-CN-0.1, P-CN-1, and P-CN-5, where the numbers represent the feeding ratio of the chromophores for P-CN-0.1, P-CN-1, and

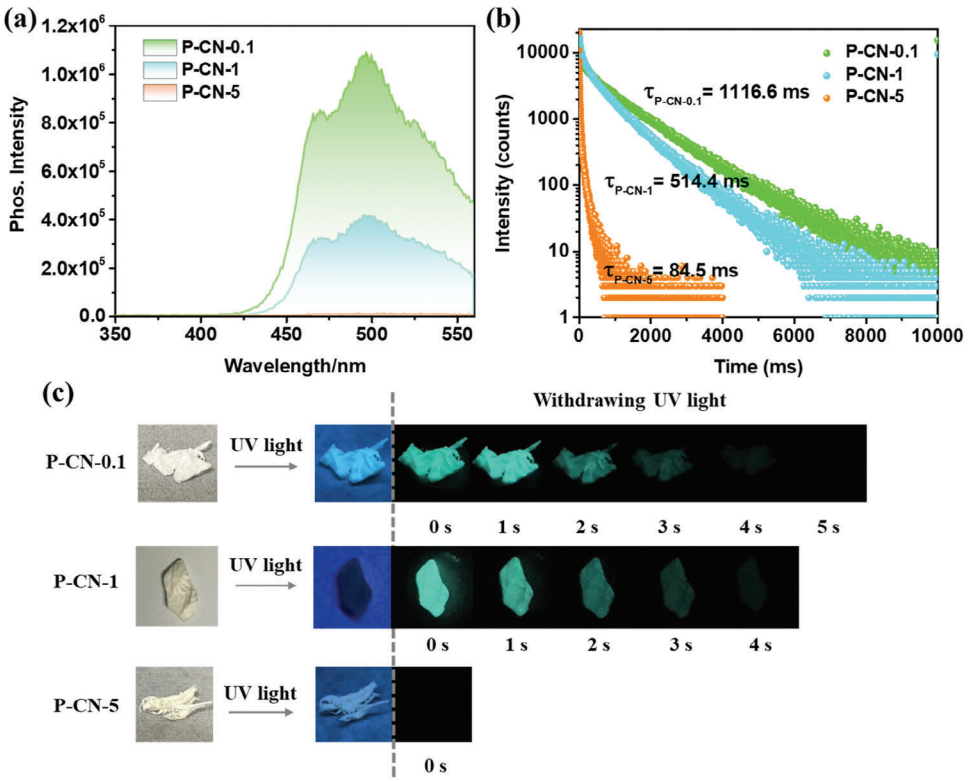

Figure 1. a) Delayed emission spectra (excitation wavelength: 286 nm, delay time: 0.1 ms), b) time-resolved photoluminescence spectra, and c) afterglow photographs (taken using 254 nm portable UV-light) of copolymers P-CN with varying degrees of substitution.

P-CN-5, respectively). Their RTP and photochromism performance were studied in detail.

The phosphorescence spectra and time-resolved decay curves revealed that P-CN-0.1, P-CN-1, and P-CN-5 exhibited varying phosphorescence intensities and lifetimes at the same emission wavelength of 495 nm. As the degree of substitution decreased, the intensity and lifetime increased (**Figure 1**a,b). The copolymer with the lowest degree of substitution, P-CN-0.1, had the strongest phosphorescence and the longest lifetime of 1116.6 ms. Correspondingly, P-CN-1 exhibited weaker phosphorescence and a shorter lifetime of 514.4 ms. When the CN–V ratio increased to 5% (P-CN-5) during copolymerization, the lifetime (84.5 ms) was sharply reduced to approximately one-tenth that of P-CN-0.1. The quantum yields also showed this trend (Table S1, Supporting Information). This is mainly attributed to the inherent photophysical characteristics of the 4-phenylpyridinium derivatives, which tend to emit phosphorescence in a single molecular state (low degree of substitution in the copolymer) rather than in an aggregated state (high degree of substitution in the copolymer), according to our previous investigation.[38,40] This is consistent with the characteristics of macrocyclic confinement inducing or enhancing phosphorescence. Furthermore, cyan afterglow was observed for both P-CN-0.1 and P-CN-1 after removing the 254 nm portable UV-light, demonstrating the long-lived nature (Figure 1c). Unexpectedly, another interesting photophysical phenomenon (photochromism) was incited when the 254 nm portable UV-light was replaced by a 275 nm UV flashlight. The 275 nm flashlight was selected as the light source because: 1) the flashlight generates a concentrated beam of light in a small region, and 2) 275 nm light is closer to the excitation wavelength of 4-phenylpyridinium derivatives containing a cyano group. After irradiating the samples for 1 min using the flashlight, the colorless solid P-CN turned dark green (**Figure 2**a; Figure S5a, Supporting Information). Meanwhile, the original flat curves in the solid UV–vis spectra became intense absorption peaks in the visible light region (416 and 636 nm; Figure 2e; Figure S5b, Supporting Information). Notably, the shades of P-CN-0.1, P-CN-1, and P-CN-5 varied under the same irradiation conditions. Compared to P-CN-0.1 and P-CN-5, P-CN-1 underwent the most obvious color change and had the strongest visible absorption, indicating that a lower or higher degree (taking 1% as a reference) of substitution of 4-phenylpyridinium derivatives was harmful to photochromic performance. Thus, a 1% molar ratio of the 4-phenylpyridinium derivatives containing a cyano group was selected for further investigation.

2.2. Effect of Substituent Sites on Photophysical Behavior

In addition to the degree of substitution, photophysical properties of organic molecules are sensitive to light sources, surroundings, and functional substitutions.[38] In this work, the light source and substitution site (i.e., the cyano group on the benzene ring of the 4-phenylpyridinium derivatives in copolymers) greatly affected the RTP and photochromic performance. Distinct phosphorescence emission and color changes were

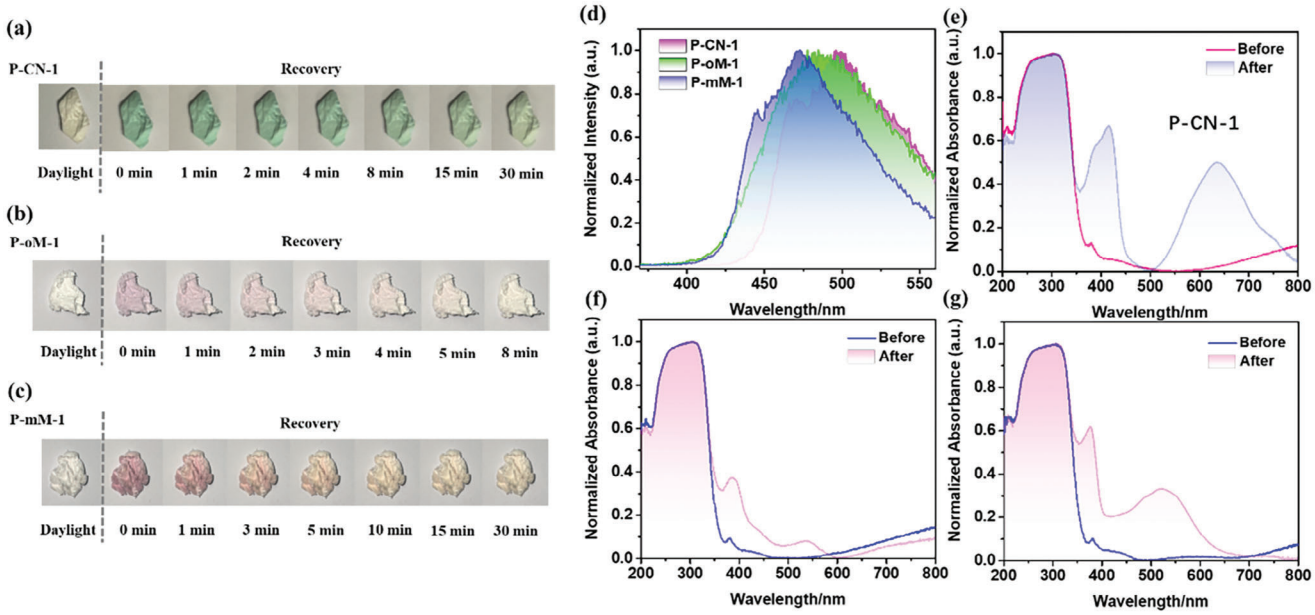

Figure 2. a–c) Photographs of P-CN-1, P-oM-1, and P-mM-1 before and after photochromism (irradiated for 1 min using a 275 nm flashlight) and finally recovering under ambient conditions; d) Delayed emission spectra of P-CN-1, P-oM-1, and P-mM-1 (excitation wavelength: 286 nm, delay time: 0.1 ms); solid UV–vis absorption spectra of (e) P-CN-1, (f) P-oM-1, and (g) P-mM-1 before and after photochromism (irradiated for 1 min using a 275 nm flashlight).

observed when the cyano group was placed at various positions (*ortho*-position: P-oM, *meta*-position: P-mM, and *para*-position: P-CN). Moreover, the strongest phosphorescence emission was observed for various copolymers when 286 nm was chosen as the excitation wavelength, even though the optimal excitation wavelength was 320 nm (Figures S6 and S7, Supporting Information). This is probably related to the fact that a higher level of excited singlet state (S_n) will induce more intersystem crossing (ISC) channels by choosing a shorter excitation wavelength, which was supported by theoretical calculations on a model molecule exhibiting multiple possible ISC pathways (Figure S8, Supporting Information).[38,41] Compared with the emission peak at 495 nm for P-CN-1, the phosphorescence peaks of P-oM-1 and P-mM-1 were obviously hypsochromatically shifted to 485 and 475 nm, respectively (Figure 2d). In addition, the average lifetimes and quantum yields of the copolymers varied according to the time-resolved photoluminescence curves and analysis of luminescence efficiency. P-mM-1 had the longest lifetime with 1056.4 ms, followed by P-oM-1 (638.9 ms), both of which exhibited long afterglow emission (Figure S9, Supporting Information). P-CN-1 exhibited the shortest lifetime (514.4 ms). The quantum yield analysis showed that fluorescence efficiency and phosphorescence efficiency were 0.99% and 5.90% for P-CN-1, respectively, 1.24% and 5.92% for P-oM-1, respectively, 1.55% and 5.30% for P-mM-1, respectively. This indicates that the phosphorescence emission prevailed over luminescence despite changing the substitution sites of the cyano group (Table S1, Supporting Information). These diverse phosphorescence properties confirmed our assumption that the substituent sites of the cyano group significantly affected the energy level of the excited triplet state and the radiative rate of phosphorescence. In addition to phosphorescence, the photochromic behavior was analogously tuned by the substitution site of the cyano group. According to the abovementioned results, a dark green appearance was formed for P-CN-1 after being irradiated for 1 min. Unexpectedly, copolymers P-mM-1 and P-oM-1 exhibited a pink appearance when the same irradiation conditions were used (Figure 2b,c). Compared with P-oM-1, P-mM-1 exhibited a more obvious change to a deeper pink color. The solid UV–vis spectrum of P-mM-1 contained characteristic peaks at 377 and 522 nm, and the spectrum of P-oM-1 exhibited peaks at 385 and 538 nm (Figure 2e,g). To the best of our knowledge, it is rare for a concisely changing substitution position to simultaneously adjust the organic RTP and photochromic performance based on light stimuli-responsiveness.

2.3. Relationship Between Photochromism and Phosphorescence

Interestingly, RTP properties are closely related to photochromism. The steady-state photoluminescence spectra and delayed emission spectra indicate that luminescence and phosphorescence sharply decreased after photochromism (**Figure 3**; Figure S10, Supporting Information). The phosphorescence intensity was 9.9, 12, and 47 fold lower for P-CN-1, P-oM-1, and P-mM-1, respectively, than that of the raw copolymers when the samples were irradiated for 1 min using a 275 nm flashlight (Figure 3a,d,g). In addition, the average lifetimes also decreased from 514.4 to 73.4 ms (P-CN-1), 638.9 to 36.8 ms (P-oM-1), and 1056.4 to 246.5 ms (P-mM-1), as shown in Figure 3b,e,h, respectively. The attenuated intensity and lifetimes were visibly observed by the naked eye via changes in the afterglow (Figure 3c,f,i, respectively). Long-lived green or cyan phosphorescence from the original copolymers faded rapidly after ceasing 254 nm UV irradiation, lasting for 3–4 s

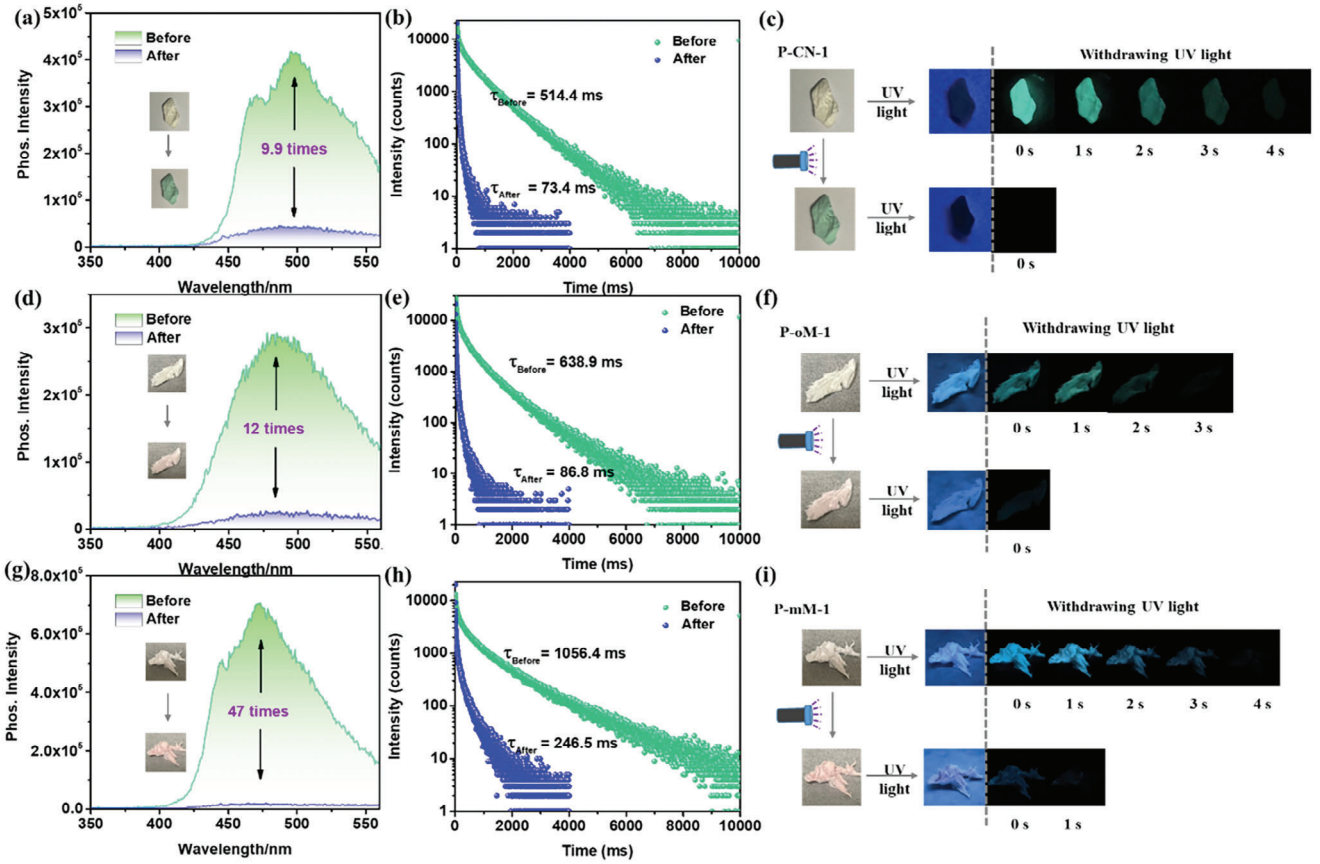

Figure 3. The delayed emission spectra (a,d,g), time-resolved photoluminescence spectra (b,e,h), and afterglow (c,f,i) photographs of (a-c) P-CN-1, (d-f) P-oM-1, and (g-i) P-mM-1 before and after photochromism using a 275 nm flashlight for 1 min (excitation wavelength: 286 nm, delay time: 0.1 ms, photographs taken from daylight and 254 nm portable UV-light).

before photochromism. This obvious attenuation indicates that the phosphorescence and photochromic behavior are two tunable photophysical properties that respond to UV-light. Achieving controllable RTP emissions is still difficult in phosphorescent materials owing to their fragility and sensitization to their surroundings, which makes our work significant. More importantly, these organic multi-functional optical materials simultaneously exhibited tunable long-lived RTP and photochromism.

2.4. Flexible Photochromic and Phosphorescent Film

To enhance the practicality of these solid copolymers, various copolymers (containing 1% and 5% chromophores) were doped into PVA to fabricate transparent and flexible films possessing RTP and photochromism. Additionally, the cyclodextrin derivative SBCD was introduced to improve the phosphorescence efficiency through supramolecular assembly based on hydrogen bonds and electrostatic interaction. According to the delayed emission spectra, the intense RTP was retained by doping P-CN-1 or P-CN-5 into the transparent PVA films (Figures S11 and S12, Supporting Information). The strongest phosphorescence signal appeared at 495 nm when the PVA film contained 6.1 mg P-CN-1 or 2.9 mg P-CN-5, indicating that an excessive amount of the copolymers stifled phosphorescence emission (Figures S11d and S12d, Supporting Information). Compared with P-CN-1, the lower doping ratio of P-CN-5 also indicated that the phosphorescence was mainly affected by the amounts of 4-phenylpyridinium derivatives, but not by the mass of the copolymer. The almost unchanged lifetimes with increasing mass of P-CN-1 or P-CN-5 demonstrated similar radiative rates of excited electrons from the triplet state in the microenvironments constructed by acrylamide copolymers and PVA (Figures S11c,e and S12c,e, Supporting Information). Compared with the lifetimes of the parent copolymers, those of P-CN-1 (514.4 ms), P-oM-1 (638.9 ms), and P-mM-1 (1056.4 ms) changed to 736.2, 610.3, and 953.6 ms, respectively, after assembling with PVA (Figures S9 and S13, Supporting Information). Meanwhile, the lifetimes of copolymers containing ≈5% 4-phenylpyridinium derivatives were also greatly improved, from 84.5 to 523.6 ms for P-CN-5, 144.0 to 376.4 ms for P-oM-5, and 267.7 to 573.0 ms for P-mM-5 (Figure 1b; Figure S14, Supporting Information). Two main reasons can explain this extraordinary enhancement: 1) the abundant hydrogen bonds from PVA further inhibit nonradiative decay (vibration, rotation, etc.), and 2) doping effects further dilute 4-phenylpyridinium derivatives and effectively prevent aggregation between chromophores. This further demonstrates

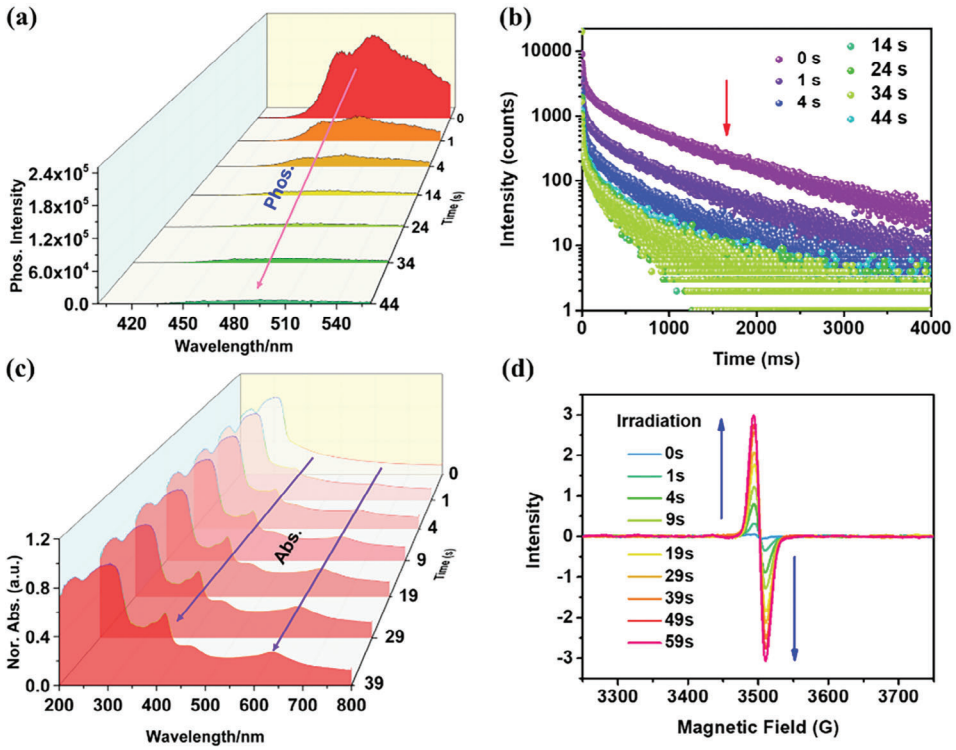

Figure 4. a) Delayed emission spectra (excitation wavelength: 286 nm; delay time: 0.1 ms); b) time-resolved photoluminescence spectra (@495 nm); c) solid UV–vis absorption spectra; and d) ESR spectra of curled P-CN-1/SBCD+PVA film with increasing irradiation time using a 275 nm flashlight.

the significance of a single-molecule environment in achieving phosphorescence emission of 4-phenylpyridinium derivatives. By adding the macrocyclic compound SBCD, aggregation among the chromophores was further suppressed owing to the formation of supramolecular assemblies based on electrostatic interaction between the 4-phenylpyridinium derivatives in the copolymers and SBCD. Transmittance measurements showed that copolymers with a high degree of substitution (≈5%) were easier to assemble with SBCD containing numerous negative charges, because they contained more positive charges than that of 1% copolymers (Figures S15 and S16, Supporting Information). As a result, the lifetimes of P-CN-5, P-oM-5, and P-mM-5 were extended to 606.7, 472.6, and 842.0 ms, further enriching the diverse room-temperature phosphorescence performance (Figure S17, Supporting Information). Considering the excellent improvement in the lifetime of P-mM-5 by assembling with SBCD, we further investigated the effect of the doping mass of P-mM-5 on the luminescence efficiency of the supramolecular films. Although there was no obvious increase, the decrease in the phosphorescence quantum yield was extremely slow as the mass of P-mM-5 increased, indicating the extraordinary assembling effect of SBCD (Table S2, Supporting Information). However, similar intensities and lifetimes were observed for P-CN-1, P-oM-1, and P-mM-1 in the PVA films with or without SBCD (Figure S18, Supporting Information), which was in agreement with the inconspicuous assembly between SBCD and 1% 4-phenylpyridinium derivatives in copolymers, as observed in transmittance spectra. Regardless of the degree of substitution, the supramolecular films exhibited excellent flexibility (Figure S19, Supporting Information).

Making copolymers into films not only facilitated the phosphorescence lifetimes but also maintained the excellent photoresponsiveness. The phosphorescence intensity and lifetimes were reduced, and the green or pink colors appeared quickly after irradiating the colorless, transparent copolymer/PVA films or copolymers+SBCD/PVA films using a 275 nm flashlight. Considering the various films in which substitution position, degree of substitution, ratio of copolymers to PVA, and supramolecular assembly were controlled, the diverse phosphorescence intensities and lifetimes were further enriched under photoresponsiveness (Figure S20–S23, Supporting Information). However, compared with solid copolymers, which exhibit local photochromism on the surface of (UV-light cannot penetrate solid copolymers), flexible supramolecular films can more readily perform overall photochromism owing to their excellent transparency. In addition, the flexible transparent films exhibited shorter response times to UV irradiation (only a few seconds). Using copolymers+SBCD/PVA as an example, a deeper investigation was performed. The delayed emission spectra demonstrated that the characteristic peaks at 495 nm for P-CN-1+SBCD/PVA were reduced gradually as a result of prolonged irradiation (**Figure** 4a; Figure S24, Supporting Information). It is noteworthy that the intensity initially weakened sharply when the films were irradiated for <14 s, and then decreased slowly with continuously increasing irradiation time from 14 s to 44 s. Similar changes are observed for P-oM-1+SBCD/PVA and P-mM-1+SBCD/PVA (Figure S25, Supporting Information).

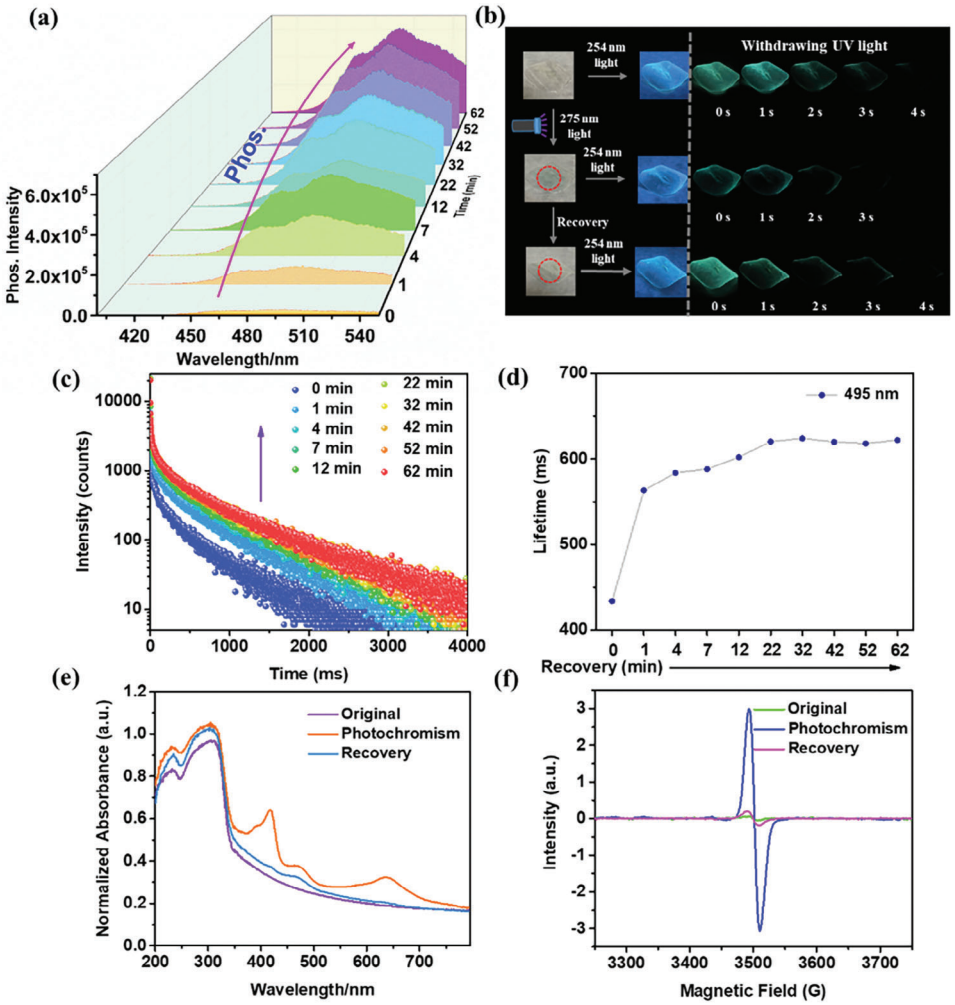

Figure 5. a) Delayed emission spectra (excitation wavelength: 286 nm, delay time: 0.1 ms), c) time-resolved photoluminescence spectra, and d) corresponding average lifetimes of P-CN-1/SBCD+PVA photochromic film after recovery at 120 C for varying times (light source: a 275 nm flashlight; irradiation time: 10 s). b) Afterglow photographs, e) solid UV–vis absorption spectra, and f) ESR spectra of P-CN-1/SBCD+PVA film before and after photochromism and recovery through heating.

In the meantime, the time-resolved photoluminescence spectra revealed the same trend, where the lifetimes of P-CN-1+SBCD/PVA, P-oM-1+SBCD/PVA, and P-mM-1+SBCD/PVA gradually declined to 356.9, 407.5, and 434.7 ms, respectively, before the irradiation time reached 14 s, and finally slowly declined or remained constant in the range of 14–44 s (Figure 4b; Figures S26 and S27, Supporting Information). Such a large attenuation within tens of seconds demonstrates that the phosphorescence of the flexible films is extremely sensitive to UV irradiation and can quickly respond to UV stimuli, which is a significant foundation for stimuli-responsive materials in practical applications. By contrast, new characteristic peaks appeared in the visible region and were gradually enhanced (416 and 636 nm for P-CN-1+SBCD/PVA; 390 and 538 nm for P-oM-1+SBCD/PVA; and 377 and 518 nm for P-mM+SBCD/PVA) in the solid UV–vis absorption spectra (Figure 4c; Figure S28, Supporting Information). The phosphorescence intensity/lifetime and absorbance almost reached their minimum and maximum values simultaneously when the irradiation time was ≈20 s, strongly indicating close relationship between RTP and photochromism. This antagonistic change, dependent on irradiation time, indicated a dynamic variation in the structure of the 4-phenylpyridinium derivatives. The photochromic structure was continuously formed when the irradiation time was <20 s, accompanied by a reduction in the phosphorescent structure. When the irradiation time exceeds 20 s, the dynamic changes cease. The absorbance, phosphorescence intensity, and lifetime remained constant. According to related literature, the majority of photochromic materials without photoreactions originate from the formation of light-driving free radicals.[22,31,32] This is also applicable to this work. As shown in the electron spin resonance (ESR) spectra of the parent copolymers and flexibly transparent films, no signals were apparent before photochromism, and strong radical signals appeared after photochromism (Figure 4d; Figures S29 and S30, Supporting Information). A similar trend was observed in the ESR spectra of the flexible films, which were responsive to irradiation time, further validating the conversion of these dynamic structures. The response time of the ESR spectra was significantly affected by

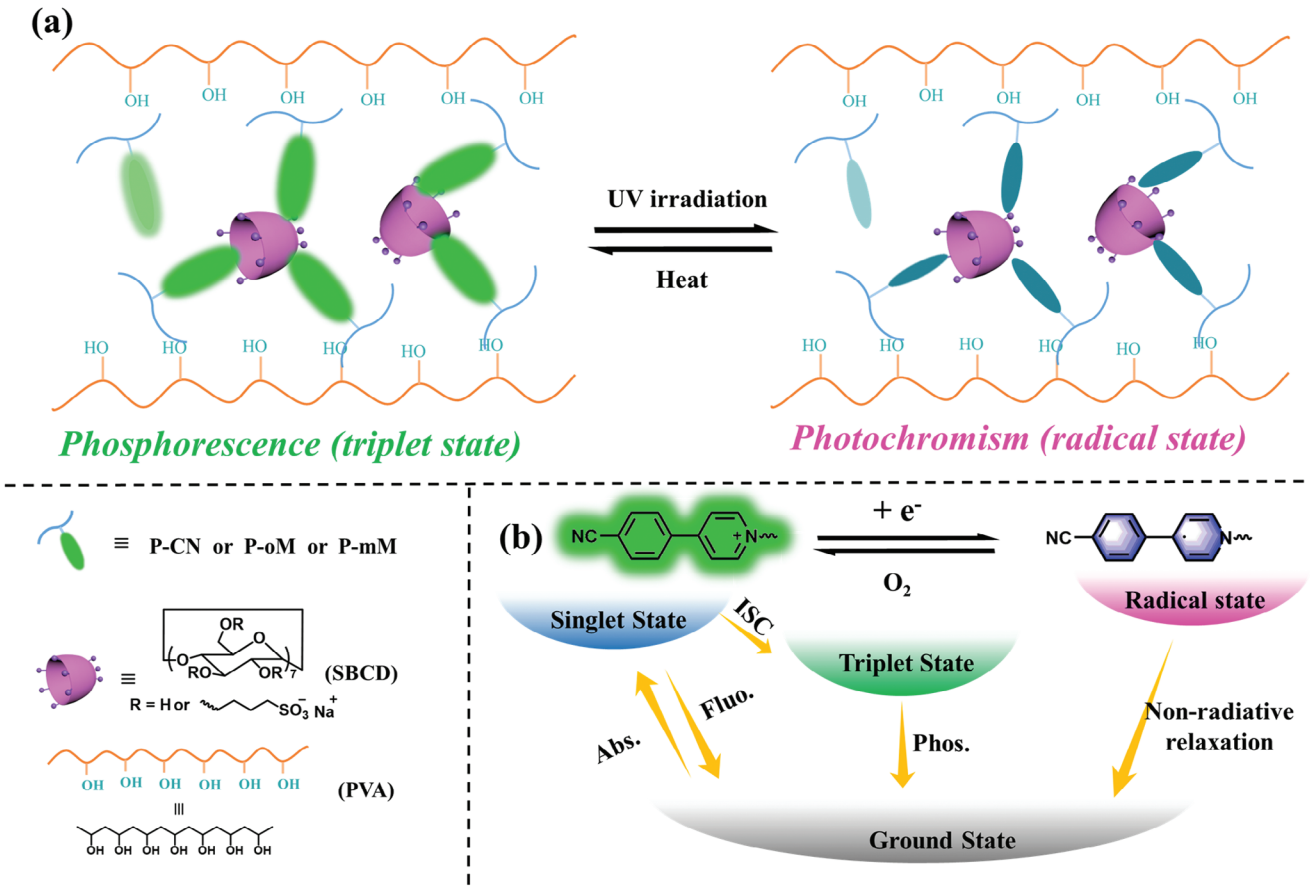

Figure 6. a) A possible assembling model, and b) energy level plots and mechanism of reversible phosphorescence and photochromism.

the testing method. The monolayer film showed similar response times to the absorption and emission spectra, further demonstrating the close relationship between the photophysical behavior and radicals (Figure S31, Supporting Information). The curled film required a longer response time because the internal films required longer periods of light to promote the formation of free radicals (Figure 4d; Figures S29 and S30, Supporting Information).

Photochromic processes can also be performed under sunlight. When the films were exposed to sunlight, a colorful appearance was observed within a few minutes, similar to the photochromism induced by the 275 nm UV flashlight (Figures S32–S34, Supporting Information). It is well-known that UV radiation from sunlight is harmful to humans. This responsiveness to sunlight makes it possible to apply these materials as UV protective films (for sunglasses, car windows, etc.) or to measure the intensity of UV rays in sunlight. The control groups showed that the individual PVA film and SBCD+PVA film could not induce color changes, proving that the photochromism originated from the acrylamide copolymers with 4-phenylpyridinium derivatives containing a cyano group. Notably, this interesting photophysical process is reversible, and the decreased phosphorescence and appearance of the films can be readily recovered by heating. In the delayed spectra, the phosphorescence intensity of the photochromic samples gradually increased with prolonged heating up to 1 h (**Figure 5a**; Figure S35, Supporting Information). Meanwhile, the average lifetimes were prolonged and finally remained unchanged (Figure 5c,d; Figure S36, Supporting Information). Correspondingly, the radical signals in the ESR spectra and the absorption peaks in the visible light region caused by photochromism almost disappeared (Figure 5e,f; Figure S37 and S38, Supporting Information). Colorless films with intense RTP were obtained. This reversible photochromic and recovery process can be repeated many times under a light stimuli (a 275 nm flashlight or sunlight) and heat, which can be recognized clearly by the naked eye through the attenuation and extension of phosphorescent afterglows (Figure 5b; Figure S39–S41, Supporting Information). Part of this loss may be attributed to the inevitable quenching of active, long-lived free radicals in the cyclic processes. Notably, the varying brightness of the sun affects the degree of photochromism.

2.5. Mechanism of Stimuli-Responsive Photochromism and Phosphorescence

Taken together, these results suggest a possible mechanism for reversible supramolecular RTP and photochromic performance (**Figure 6a**). 4-Phenylpyridinium derivatives containing a cyano group, as organic chromophores in copolymers or flexible supramolecular films, are phosphorescent by nature and

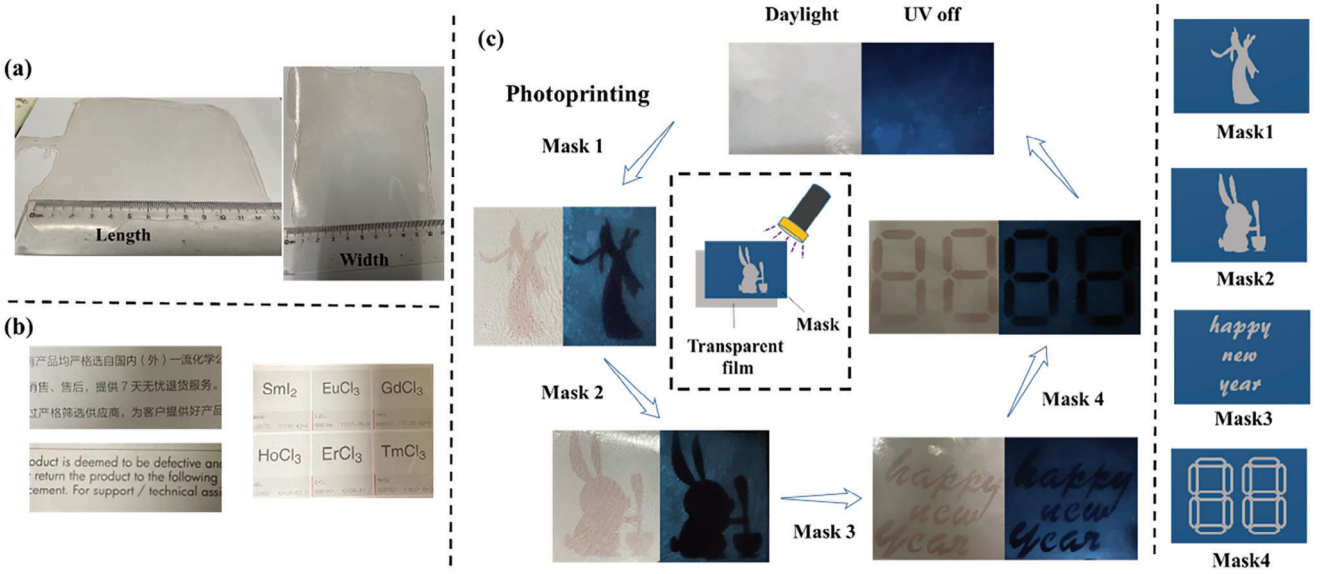

Figure 7. a) The flexible P-mM-1/SBCD+PVA film with 0.1 m (width) × 0.13 m (length); b) The words, Chinese characters and chemical formula on paper after being covered by P-mM-1/SBCD+PVA flexible film; c) Cyclic photoprinting experiments through UV-responsive photochromism and phosphorescence based on P-mM-1/SBCD+PVA film (left: photographs under daylight; right: photographs after ceasing 254 nm portable light; light source for photochromism: 275 nm flashlight).

enable the emission of robust RTP with long lifetimes under short and weak UV-light stimuli (such as the 254 nm portable UV-light). When portable UV-light is replaced with a flashlight, the phosphorescent 4-phenylpyridinium derivatives obtain an electron and are reduced to an organic radical state capable of absorbing visible light (colored appearance), the latter of which is non-phosphorescent or emits weak phosphorescence (Figure 6b). Therefore, the presence or absence of free radicals is the key to tuning the RTP and photochromism. This was validated by the decrease and recovery of phosphorescence under intense UV irradiation and heat conditions, accompanied by the occurrence and disappearance of free radical signals. When cyano is a *para* substituent, it can stabilize the radical through electron delocalization, thus enabling it to absorb light with a lower energy (≈636 nm). However, *meta* substituent or a large steric hindrance from *ortho* substituent inhibits electron delocalization, corresponding to a larger energy-level difference (≈530 nm). The almost unchanged peaks of the original and recovered copolymers in the ^{1}H NMR spectra indicated no dimerization among the 4-phenylpyridinium derivatives under 275 nm UV irradiation (Figures S42–S44, Supporting Information). By replacing the 275 nm flashlight with a 365 nm flashlight, no obvious photochromic behavior was observed (Figure S45, Supporting Information), indicating that the energy of the 365 nm light source was not sufficient to support the generation of radicals. Moreover, direct irradiation of the copolymer in aqueous solution did not induce photochromic performance, proving that the formation of radicals requires a rigid environment (Figure S46, Supporting Information). According to the related literature,[42,43] pyridinium can gain an electron and be reduced to an organic radical stabilized by the cyano group,[44] which is oxidized back to pyridinium by oxygen (Figure 6b). This agrees with the experimental results, in which oxygen or nitrogen could accelerate or postpone the recovery of phosphorescence and disappearance of photochromism, respectively (Figure S47, Supporting Information). Thus, we deduced that the photochromic samples can recover under natural conditions, mainly owing to oxygen in the atmosphere. On the other hand, the rigid environment imposed by the multiple hydrogen bonds in the acrylamide copolymers and PVA, as well as single-molecule environment, are the other crucial factors. No phosphorescence or photochromism was observed when the number of hydrogen bonds was reduced to limit the inhibition of various nonradiative pathways (vibration, rotation, collision, etc.) (Figure S48, Supporting Information). The weak phosphorescence and lack of photochromism of the monomers also support this viewpoint (Figures S2–S4, Supporting Information). Direct doping of the monomers and SBCD into PVA to complement the loss of hydrogen bonds could induce similar photochromic phenomena; however, the phosphorescence and photochromism were far less intense than those of the copolymer/SBCD+PVA (Figures S49 and S50, Supporting Information). These results highlight the importance of copolymerization in realizing RTP and photochromism by effectively avoiding the aggregation of 4-phenylpyridinium derivatives and suppressing multiple non-radiative deactivations. Furthermore, the selection of a carboxyl pillar[5]arene (WP5A) and negatively charged polymer P-COO^{-}Na^{+} demonstrated the significance of SBCD. The weak phosphorescence induced by WP5A suggested that SBCD had a superior enhancement effect on the copolymers (P-CN-5, P-mM-5, and P-oM-5) (Figures S51 and S52, Supporting Information). Nevertheless, the linear polymer P-COO^{-}Na^{+} induced copolymer precipitation despite the addition of a small amount (0.01 mg) to the copolymer, which was detrimental to the transparent films (Figure S53, Supporting Information). The XRD spectra showed an unchanged amorphous structure before and after photochromism, suggesting that UV irradiation had no effect on the structure of the films (Figure S54, Supporting Information).

2.6. Photoprinting Application

These flexible supramolecular materials exhibit excellent transparencies and can be prepared over large areas. As demonstrated by a simple scale-up experiment, a transparent film with dimensions of 0.1 m (width) × 0.13 m (length) was successfully obtained by proportionally increasing the amounts of the copolymers, SBCD, and PVA (**Figure** 7a). The quality and transparency of the film did not decrease with an increase in the amount of raw material, and various words and characters were clearly visible, even though they were covered by the supramolecular film (Figure 7b). These traits indicate that this type of material can be easily and appropriately produced industrially. Harnessing the characteristics of UV-responsive photochromism and phosphorescence, these materials were applied to repeatable photoprinting. Diverse digits, words, and patterns were written and printed on flexible films using a UV flashlight through the rational design of the mask (Figure 7c). Owing to the photochromism and the stimuli-responsiveness of the phosphorescence afterglow, the printed patterns could be recognized by the naked eye under daylight or after removing the portable 254 nm light, greatly enhancing the ornamental value of these photoprinting artworks.

3. Conclusion

In summary, various acrylamide copolymers with 4-phenylpyridinium containing a cyano group exhibited excellent RTP emission and photochromic behaviors. By tuning the substitution site of the cyano group on 4-phenylpyridinium or the molar ratio of 4-phenylpyridinium during copolymerization, the resulting copolymers showed diverse phosphorescence lifetimes, phosphorescence intensities, and colorful photochromism (dark green and pink). These phosphorescence lifetimes were further prolonged after coassembly with SBCD and PVA to form flexible transparent films. Intriguingly, the RTP properties (including intensity and lifetime) and photochromic behavior are tunable and can reversibly respond to UV irradiation and heat. Furthermore, conversion of these solid copolymers into films endows these phosphorescent and photochromic materials with huge potential for applications such as UV-blocking films (sunglasses), flexible luminescent electronic devices, photoprinting techniques, and smart UV-sensing and detection. Thus, this work not only realizes a reversibly tunable room-temperature phosphorescent and photochromic system but also provides a feasible pathway for multi-functional, stimuli-responsive smart optical materials.

4. Experimental Section

Preparation of 60 mg mL^{-1} PVA Solution: PVA (6.0001 g) and 100 mL deionized water were added into 250 mL round-bottom flask, which was stirred under reflux condition. After PVA was dissolved completely, the hot solution was filtered immediately by a syringe filter with aperture of 800 nm to afford the stock solution.

Preparation of Flexibly Transparent Films Copolymers + PVA: Copolymers (6.0 mg) (P-CN-1 or P-oM-1 or P-mM-1) or 3.0 mg copolymers (P-CN-5 or P-oM-5 or P-mM-5) were dissolved in deionized water (0.5 mL). Then, 1 mL 60 mg mL^{-1} PVA solution (solvent: deionized water) was added in the abovementioned solution, which was further treated by ultrasonic condition. After mixing completely, the resulting copolymer/PVA solution was dropped on glass matrix. The sample was placed in constant temperature drying oven at 70 °C for 4 h, and then 120°C for 2 h to get rid of water. As a result, a flexibly transparent film was successfully obtained.

Preparation of Flexibly Transparent Films Copolymers/SBCD+PVA: Copolymers (6.0 mg) (P-CN-1 or P-oM-1 or P-mM-1) or 3.0 mg copolymers (P-CN-5 or P-oM-5 or P-mM-5) were dissolved in deionized water (0.5 mL). Then, SBCD (0.5 equivalent to chromophores in copolymers, molar ratio) and 1 mL 60 mg mL^{-1} PVA solution were separately added to the abovementioned solution, which was further treated by ultrasonic condition. After mixing completely, the resulting copolymer/PVA solution was dropped on glass matrix. The sample was placed in a constant temperature drying oven at 70 °C for 4 h, and then 120 °C for 2 h to get rid of water. As a result, a flexibly transparent film was successfully obtained.

Note: Less amount of SBCD (such as: 0.1 eq.) will promote copolymers containing high substitution degree of 4-phenylpyridinium derivatives to precipitate obviously and more amount of SBCD (such as: 1.0 eq.) will make the resulting films loss flexibility and become fragile. Therefore, 0.5 eq. SBCD to chromophore is a compromised molar ratio to prepare flexible supramolecular films. Although there is also some turbid liquid for P-CN-5 or P-oM-5 or P-mM-5 when adding SBCD, the resulting films are still transparent after removing solvent.

Preparation of Flexibly Transparent Films Monomers + PVA: With CN–V+PVA as an example, CN–V (equivalent to the molar ratio of chromophores in 6.0 mg P-CN-1) was dissolved in 0.5 mL deionized water, and then added 1 mL 60 mg mL^{-1} PVA solution (solvent: deionized water). After mixing completely, the resulting CN–V+PVA solution was dropped on glass matrix. The sample was placed in constant temperature drying oven at 70 °C for 4 h, and then 120 °C for 2 h to get rid of water. As a result, a flexibly transparent film was successfully obtained. Similar method was used to prepare oM–V+PVA and mM–V+PVA.

Preparation of Flexibly Transparent Films Monomers/SBCD + PVA: With CN–V/SBCD+PVA as an example, CN–V (equivalent to CN–V) and SBCD (0.5 equivalent to the molar ratio of chromophores in 6.0 mg P-CN-1) were dissolved in 0.5 mL deionized water, and then 1 mL 60 mg mL^{-1} PVA solution (solvent: deionized water). After mixing completely, the resulting CN–V/SBCD+PVA solution was dropped on glass matrix. The sample was placed in constant temperature drying oven at 70 °C for 4 h, and then 120 °C for 2 h to get rid of water. As a result, a flexibly transparent film was successfully obtained. A similar method was used to prepare oM–V/SBCD+PVA and *mM–V*/SBCD+PVA.

Photoprinting Experiment: Copolymer P-mM-1 (182.4 mg) was dissolved in 13.21 mL deionized water under ultrasonic condition. Then, 1.79 mL SBCD (10^{-2} M, 0.5 equivalent to chromophores in P-mM-1, molar ratio) was added into copolymer solution. After forming supramolecular assembly, 30 mL PVA solution (60 mg mL^{-1}) was introduced, which was further mixed under ultrasonic condition. The mixed solution was dropped on glass matrix (20 cm × 20 cm) and dried at 50 °C overnight and following 100 °C for 1 h. The resulting film was further dried in vacuum oven at 50 °C for 6 h. Covering the film with mask (rabbit, word or digits, and so on), the blank area was irradiated by 275 nm flashlight to afford the photoprinting patterns. The photoprinting film could be dissolved in deionized water under reflux condition and the transparent film could be prepared again according to the abovementioned procedures. This process could be repeated many times to give different photoprinting patterns by using diverse masks.

Compound CN–N: The compound CN−N was prepared according to the previous work.[38] ^{1}H NMR (400 MHz, $CDCl_3$, ppm) δ: 8.74 (d, J = 6.0 Hz, 2H), 7.81 (d, J = 8.4 Hz, 2H), 7.75 (d, J = 8.4 Hz, 2H), 7.51 (d, J = 6.1 Hz, 2H).

Compound oM–N: Pyridin-4-ylboronic acid (321.2 mg, 2.6 mmol, 1.2 eq.), 2-bromobenzonitrile (392.0 mg, 2.15 mmol, 1.0 eq.), sodium carbonate (685.2 mg, 6.5 mmol, 3.0 eq.) and tetrakis(triphenylphosphine)palladium (200.3 mg, 0.17 mmol, 0.08 eq) were placed in a 100 mL round-bottom flask and dioxane/H_2O were used as mixed solvent. The reaction was performed on a magnetic agitator under reflux condition for 11.5 h. After the reaction was finished, the solvents were removed through a rotary evaporator. The crude solid was washed with water and dichloromethane (1/1, 100 mL 100 mL^{-1}) and the

organic phase was collected. The water phase was washed with 50 mL dichloromethane for three times. The organic phase was integrated and purified by column chromatography (petroleum ether/ethyl acetate = 10:3). ^{1}H NMR (400 MHz, $CDCl_3$, ppm) δ 8.76 (d, J = 6.1 Hz, 2H), 7.82 (d, J = 7.0 Hz, 1H), 7.71 (t, J = 7.7 Hz, 1H), 7.55 (m, 2H), 7.49 (d, J = 6.1 Hz, 2H); ^{13}C NMR (100 MHz, $CDCl_3$, ppm) δ 149.27, 144.55, 141.44, 133.05, 132.20, 128.78, 127.95, 122.29, 116.91, 110.13; HRMS (ESI) (m/z): $[M]^+$ calcd. for oM–N, 180.07; found, 181.0761.

Compound CN–V: The compound CN–V was prepared according to the previous work.[38] ^{1}H NMR (400 MHz, CD_3OD, ppm) δ: 9.11 (d, J = 6.7 Hz, 2H), 8.47 (d, J = 6.7 Hz, 2H), 8.15 (d, J = 8.4 Hz, 2H), 7.99 (d, J = 8.4 Hz, 2H), 7.56 (d, J = 8.2 Hz, 2H), 7.51 (d, J = 8.3 Hz, 2H), 6.77 (dd, J = 17.6, 11.0 Hz, 1H), 5.88–5.83 (m, 3H), 5.32 (d, J = 11.0 Hz, 1H); ^{13}C NMR (100 MHz, CD_3OD, ppm) δ 156.58, 146.25, 140.82, 139.60, 137.13, 134.56, 133.87, 130.56, 130.24, 128.42, 127.23, 118.84, 116.69, 116.08, 64.97

Compound oM–V: The compound oM–V was prepared similar to the synthesis of compound CN–V. Scheme S1 (Supporting Information) includes the corresponding synthetic route. ^{1}H NMR (400 MHz, CD_3OD, ppm) δ: 9.21 (d, J = 6.8 Hz, 2H), 8.41 (d, J = 6.7 Hz, 2H), 8.02 (d, J = 7.7 Hz, 1H), 7.93 (t, J = 7.7 Hz, 1H), 7.87 (d, J = 7.0 Hz, 1H), 7.80 (t, J = 8.2 Hz, 1H), 7.57 (s, 4H), 6.78 (dd, J = 17.6 Hz, 10.9 Hz, 1H), 5.92 (s, 2H), 5.87 (d, J = 17.6 Hz, 1H), 5.33 (d, J = 10.9 Hz, 1H); ^{13}C NMR (100 MHz, CD_3OD, ppm) δ 156.31, 146.17, 140.85, 139.65, 137.14, 135.76, 135.22, 133.72, 132.76, 131.81, 130.73, 129.45, 128.45, 118.29, 116.12, 112.31, 65.28; HRMS (ESI) (m/z): $[M\text{-}Cl]^+$ calcd for CN–V, 297.14; found, 297.1389.

Compound mM–V: The compound mM–V was prepared similar to the synthesis of compound CN–V. Scheme S2 (Supporting Information) includes the corresponding synthetic route. ^{1}H NMR (400 MHz, CD_3OD, ppm) δ: 9.11 (d, J = 6.7 Hz, 2H), 8.48 (d, J = 6.7 Hz, 2H), 8.41 (s, 1H), 8.29 (d, J = 8.1 Hz, 1H), 8.02 (d, J = 7.8 Hz, 1H), 7.82 (t, J = 7.9 Hz, 1H), 7.56 (d, J = 8.2 Hz, 2H), 7.52 (d, J = 8.2 Hz, 2H), 6.77 (dd, J = 17.6 Hz, J = 11.0 Hz, 1H), 5.86 (m, 3H), 5.33 (d, J = 10.9 Hz, 1H); ^{13}C NMR (100 MHz, CD_3OD, ppm) δ 154.86, 144.76, 139.39, 135.68, 135.28, 134.98, 132.42, 132.25, 131.63, 130.62, 129.12, 126.98, 125.57, 117.36, 114.65, 113.83, 63.49; HRMS (ESI) (m/z): $[M\text{-}Cl]^+$ calcd for CN–V, 297.14; found, 297.1393.

General Synthesis of the Polymers: P-CN-1 was prepared as a model.[38] In 6.0 mL anhydrous DMF under dark and argon atmosphere, P-CN-1 was prepared by copolymerization of CN–V (33.4 mg, 0.1 mmol, 1.0 eq) and acrylamide (695.8 mg, 9.8 mmol, 98.0 eq.) with 2,2'-azobis(2-methylpropionitrile) (AIBN) (16.0 mg) as radical initiator at 65°C for 12 h. After cooling, the crude solid obtained through filtration was dissolved by deionized water and the mixture was dialyzed (cutoff = 2000) against water for 3d. The resulting solution was lyophilized and further dried under vacuum to give solid polymer. Similar method was performed to afford other polymers (True degree of substitution characterized by ^{1}H NMR spectra: 0.10% for P-CN-0.1, 1.1% for P-CN-1, 0.97% for P-oM-1, 1.0% for P-mM-1, 5.4% for P-CN-5, 5.8% for P-oM-5, 5.4% for P-mM-5.).

Supporting Information

Supporting Information is available from the Wiley Online Library or from the author.

Acknowledgements

This work was financially supported by the National Natural Science Foundation of China (grant 22131008) and the Fundamental Research Funds for the Central Universities, Nankai University. The authors thank the Haihe Laboratory of Sustainable Chemical Transformations for the financial support.

Conflict of Interest

The authors declare no conflict of interest.

Data Availability Statement

The data that support the findings of this study are available in the supplementary material of this article.

Keywords

electrostatic assemblies, photochromism, reversible optical properties, room-temperature phosphorescence, stimuli-responsiveness

Received: November 30, 2023
Revised: January 28, 2024
Published online: February 9, 2024

[1] Y. Shi, W. Su, F. Yuan, T. Yuan, X. Song, Y. Han, S. Wei, Y. Zhang, Y. Li, X. Li, L. Fan, *Adv. Mater.* **2023**, *35*, 2210699.
[2] S. Y. Yang, Y. K. Qu, L. S. Liao, Z. Q. Jiang, S. T. Lee, *Adv. Mater.* **2022**, *34*, 2104125.
[3] Z. Xie, X. Zhang, Y. Xiao, H. Wang, M. Shen, S. Zhang, H. Sun, R. Huang, T. Yu, W. Huang, *Adv. Mater.* **2023**, *35*, 2212273.
[4] S. Cai, X. Yao, H. Ma, H. Shi, Z. An, *Aggregate* **2023**, *4*, e320.
[5] H. Sun, L. Zhu, *Aggregate* **2023**, *4*, e253.
[6] S. Yang, W. Dai, W. Zheng, J. Wang, *Coord. Chem. Rev.* **2023**, *475*, 214913.
[7] Q. Zhou, C. Yang, Y. Zhao, *Chem* **2023**, *9*, 2446.
[8] H. E. Hackney, D. F. Perepichka, *Aggregate* **2022**, *3*, e123.
[9] B. Ding, X. Ma, H. Tian, *Acc. Mater. Res.* **2023**, *4*, 827.
[10] X. Yan, H. Peng, Y. Xiang, J. Wang, L. Yu, Y. Tao, H. Li, W. Huang, R. Chen, *Small* **2022**, *18*, 2104073.
[11] X.-K. Ma, Y. Liu, *Acc. Chem. Res.* **2021**, *54*, 3403.
[12] X. Ma, J. Wang, H. Tian, *Acc. Chem. Res.* **2019**, *52*, 738.
[13] M. Huo, X.-Y. Dai, Y. Liu, *Small* **2022**, *18*, 2104514.
[14] X. Feng, X. Wang, C. Redshaw, B. Z. Tang, *Chem. Soc. Rev.* **2023**, *52*, 6715.
[15] Z. Wang, T. Li, B. Ding, X. Ma, *Chin. Chem. Lett.* **2020**, *31*, 2929.
[16] B. Xu, Y. Jia, H. Ning, Q. Teng, C. Li, X. Fang, J. Li, H. Zhou, X. Meng, Z. Gao, X. Wang, Z. Wang, F. Yuan, *Small* **2023**, https://doi.org/10.1002/smll.202304958.
[17] H. C. Byron, C. Swain, P. Paturi, P. Colinet, R. Rullan, V. Halava, T. L. E Bahers, M. Lastusaari, *Adv. Funct. Mater.* **2023**, *33*, 2303398.
[18] C. C. Ko, V. W. W. Yam, *Acc. Chem. Res.* **2018**, *51*, 149.
[19] J. Xu, H. Volfova, R. J. Mulder, L. Goerigk, G. Bryant, E. Riedle, C. Ritchie, *J. Am. Chem. Soc.* **2018**, *140*, 10482.
[20] J. L. Zhao, M. H. Li, Y. M. Cheng, X. W. Zhao, Y. Xu, Z. Y. Cao, M. H. You, M. J. Lin, *Coord. Chem. Rev.* **2023**, *475*, 214918.
[21] Z. Li, X. Zeng, C. Gao, J. Song, F. He, T. He, H. Guo, J. Yin, *Coord. Chem. Rev.* **2023**, *497*, 215451.
[22] Y.-J. Ma, G. Xiao, X. Fang, T. Chen, D. Yan, *Angew. Chem., Int. Ed.* **2023**, *62*, 202217054.
[23] G. Huang, Q. Xia, W. Huang, J. Tian, Z. He, B. S. Li, B. Z. Tang, *Angew. Chem., Int. Ed.* **2019**, *58*, 17814.
[24] H. Zhang, Q. Li, Y. Yang, X. Ji, J. L. Sessler, *J. Am. Chem. Soc.* **2021**, *143*, 18635.
[25] T. Zhang, X. Y. Lou, X. Li, X. Tu, J. Han, B. Zhao, Y. W. Yang, *Adv. Mater.* **2023**, *35*, 2210551.
[26] Y. Chen, Y. R. Lee, W. Wang, Y. Fang, S. Lu, J. Han, X. Chen, M. H. Kim, J. Yoon, *Angew. Chem., Int. Ed.* **2023**, *62*, 202301765.
[27] Y. Ding, J. Guo, X. He, W. Tao, Y. Shi, J. Xu, L. Xu, M. Tang, D. Shen, H. Bi, Z. Q. Wu, K. Yang, Z. Zeng, P. Wei, *Adv. Funct. Mater.* **2023**, *33*, 2212886.
[28] H. Ito, K. Mutoh, J. Abe, *J. Am. Chem. Soc.* **2023**, *145*, 6498.

[29] A. Kometani, Y. Inagaki, K. Mutoh, J. Abe, *J. Am. Chem. Soc.* **2020**, *142*, 7995.
[30] M. Sacherer, F. Hampel, H. Dube, *Nat. Commun.* **2023**, *14*, 4382.
[31] W. Liu, J. Wang, Y. Gong, Q. Liao, Q. Dang, Z. Li, Z. Bo, *Angew. Chem., Int. Ed.* **2020**, *59*, 20161.
[32] Y. Yang, J. Wang, D. Li, J. Yang, M. Fang, Z. Li, *Adv. Mater.* **2021**, *33*, 2104002.
[33] Y. Fan, M. Han, A. Huang, Q. Liao, J. Tu, X. Liu, B. Huang, Q. Li, Z. Li, *Mater. Horiz.* **2022**, *9*, 368.
[34] B. Wu, X. Xu, Y. Tang, X. Han, G. Wang, *Adv. Opt. Mater.* **2021**, *9*, 2101266.
[35] Y. Shi, Y. Zeng, P. Kucheryavy, X. Yin, K. Zhang, G. Meng, J. Chen, Q. Zhu, N. Wang, X. Zheng, F. Jäkle, P. Chen, *Angew. Chem., Int. Ed.* **2022**, *61*, 202213615.
[36] C. Wang, Y. H. Liu, Y. Liu, *Small* **2022**, *18*, 2201821.
[37] Z. Xu, Q. T. Liu, X. Wang, Q. Liu, D. Hean, K. C. Chou, M. O. Wolf, *Chem. Sci.* **2020**, *11*, 2729.
[38] W.-W. Xu, Y. Chen, Y.-L. Lu, Y.-X. Qin, H. Zhang, X. Xu, Y. Liu, *Angew. Chem., Int. Ed.* **2022**, *61*, 202115265.
[39] X. Ma, C. Xu, J. Wang, H. Tian, *Angew. Chem., Int. Ed.* **2018**, *57*, 10854.
[40] Z. Y. Zhang, W. W. Xu, W. S. Xu, J. Niu, X. H. Sun, Y. Liu, *Angew. Chem., Int. Ed.* **2020**, *59*, 18748.
[41] J. Guo, J. Fan, L. Lin, J. Zeng, H. Liu, C. K. Wang, Z. Zhao, B. Z. Tang, *Adv. Sci.* **2019**, *6*, 1801629.
[42] M. Kathiresan, B. Ambrose, N. Angulakshmi, D. E. Mathew, D. Sujatha, A. M. Stephan, *J. Mater. Chem. A* **2021**, *9*, 27215.
[43] G. Xu, G. C. Guo, M. S. Wang, Z. J. Zhang, W. T. Chen, J. S. Huang, *Angew. Chem. Inter. Ed.* **2007**, *46*, 3249.
[44] D. Yuan, D. Huang, S. M. Rivero, A. Carreras, C. Zhang, Y. Zou, X. Jiao, C. R. McNeill, X. Zhu, C.-A. Di, D. Zhu, D. Casanova, J. Casado, *Chem* **2019**, *5*, 964.

